



HAL
open science

Modeling of dilution enthalpies within implicit-solvent models for electrolytes

Jean-Pierre Simonin

► **To cite this version:**

Jean-Pierre Simonin. Modeling of dilution enthalpies within implicit-solvent models for electrolytes. Journal of Molecular Liquids, 2024, 394, pp.123801. 10.1016/j.molliq.2023.123801 . hal-04530705

HAL Id: hal-04530705

<https://hal.sorbonne-universite.fr/hal-04530705>

Submitted on 3 Apr 2024

HAL is a multi-disciplinary open access archive for the deposit and dissemination of scientific research documents, whether they are published or not. The documents may come from teaching and research institutions in France or abroad, or from public or private research centers.

L'archive ouverte pluridisciplinaire **HAL**, est destinée au dépôt et à la diffusion de documents scientifiques de niveau recherche, publiés ou non, émanant des établissements d'enseignement et de recherche français ou étrangers, des laboratoires publics ou privés.

Modeling of dilution enthalpies within implicit-solvent models for electrolytes

Jean-Pierre Simonin^{a,*}

^a*CNRS, Laboratoire PHENIX, Sorbonne Université (Campus P.M. Curie), 4 Place Jussieu, Case 51, F-75005, Paris, France*

Abstract

This work deals with the calculation of dilution enthalpies for strong aqueous electrolyte solutions when their thermodynamic properties are described within implicit-solvent models. The solution is modeled as a collection of charged hard spheres in a continuum solvent. A new general expression is obtained that accounts for the variation of the solution permittivity, of the size of the ions, and of the specific volume of the solution, with temperature and concentration. This expression is used to compute the enthalpies of LiCl aqueous solutions at temperatures in the range of 25°C to 100°C for concentrations up to 6 mol kg⁻¹. The mean spherical approximation (MSA) model with implicit continuum solvent is employed to describe the thermodynamic properties of these solutions.

Keywords: Enthalpy, Dilution, Modeling, Electrolyte, Mean spherical approximation (MSA)

1. Introduction

The theoretical prediction of thermal effects in electrolytes is of interest in industrial processes, such as absorption refrigeration [1] (mainly using LiBr solutions), CO₂ capture [2], or when mixing electrolyte solutions in chemical reactors. The dilution of an ionic solution is an example of such a process. The thermal effect accompanying it is a versatile phenomenon [3] because it can generate a release or an absorption of heat, depending on the initial and final salt concentrations and the temperature at which the dilution is performed.

Dilution enthalpies have been extensively studied in the literature for more than a century [4, 5]. Many experiments have been carried out, mainly on aqueous solutions [6–14]. Experimental results have been described mostly with models based on the Debye-Hückel (DH) theory [6–8, 12, 14–18].

Another approach using a DH-type term is the Pitzer model [19] which offers a convenient way of representing deviations from ideality in aqueous electrolyte solutions by combining a DH contribution and a virial-type expansion in the Gibbs energy of the solution, that are both expressed in terms of molalities. The latter peculiarity advantageously avoids accounting for volume changes when the temperature is varied. Then it is easier to obtain expressions for first- or second-order derivative properties like enthalpies and heat capacities with this model. Beside these descriptions, the mean spherical approximation (MSA) model [20] has been employed in a few works for an account of electrostatic effects on heats of dilution [21–24].

*Corresponding author

Email address: jpsimonin@gmail.com. Tel. +33 144273190 (Jean-Pierre Simonin)

The DH and MSA treatments are models with implicit solvent. As such, they are developed at the McMillan-Mayer (MM) level of solutions [25] where the chemical potential of the solvent is maintained constant by applying an additional pressure (the osmotic pressure) on the solution [26]. The MM framework is a generalization to concentrated solutions of the theory of van't Hoff [27], who first highlighted the analogy between a dilute solution and a gas of solute. In contrast, dilution enthalpies are measured at constant pressure, at the Lewis-Randall (LR) level of the ‘real world’ (laboratory). When experimental quantities are represented using an implicit-solvent model, a conversion of the MM theoretical results to the LR framework must be performed in order to compare them with experimental data [28–30].

The use of a MM model to describe dilution enthalpies thus requires a suitable treatment. However, to the best knowledge of this author, it seems that, despite some preliminary work on this topic [26, 28], such a complete treatment has not been presented so far. In the few publications using the MSA, the final expression for the enthalpy was at best obtained by differentiating intermediate MSA quantities with respect to temperature, which resulted in cumbersome equations with limited physical meaning [22, 23]. An examination of the literature calls for two main remarks: (i) The passage from MM level to LR has not been included in the models describing dilution enthalpy data and, (ii) no simple and compact theoretical relation has been proposed from which values can be predicted.

The purpose of this work is first to bridge this gap, and derive general and compact expressions for the dilution enthalpies of strong electrolytes. This task was facilitated by using some fundamental work by Friedman [28], which seems to have remained unnoticed in the subsequent literature. These expressions were then used for a study of dilution enthalpies for a particular system.

The present work is organized in the following way. The theoretical aspects of the problem are developed in the next section. This includes a new general expression for the dilution enthalpy of an electrolyte solution, and a workable relation in terms of quantities at the MM level. Then, use of these relations is illustrated in the case of LiCl aqueous solutions between 25°C and 100°C for concentrations up to 6 mol kg⁻¹. In a first step, the approach involves a representation of the experimental activity and osmotic coefficients within the MSA framework, by assuming that the solution permittivity and ion sizes vary with the salt concentration and the temperature with dependence involving some adjustable parameters. In a second step, this description is used for a computation of the dilution enthalpies, and these results are compared with literature data for this quantity. Agreement between the two suggests that the procedure is thermodynamically consistent and that the expression for the enthalpy is valid.

2. Theory

2.1. Dilution enthalpies

The heat of dilution from an initial concentration to infinite dilution, which is equal to but of opposite sign of the relative apparent molal heat content, L_ϕ , is not a directly measurable quantity [12]. The heat measured experimentally is a difference, ΔL_ϕ , observed when going from an initial to a final finite concentration. Values for L_ϕ have been generally obtained by extrapolation of low-concentration data to zero concentration by using the extended DH equation [31].

The heat of dilution per mole of solute in the process going from a solution of molality m_1 to one of molality m_2 is [19]

$$\Delta H_d(m_1 \rightarrow m_2) = L_\phi(m_2) - L_\phi(m_1) \tag{1}$$

in which L_ϕ is the apparent relative molal enthalpy,

$$L_\phi = \frac{1}{n} \frac{\partial(G^{LR}/T)}{\partial(1/T)} \Big|_{P,m} \quad (2)$$

where n is the number of moles of solute, G^{LR} is the excess Gibbs energy of solution per kilogram of solvent, at LR level (that of the experiment) [32],

$$G^{LR} = \nu n R T (1 - \phi^{LR} + \ln \gamma^{LR}) \quad (3)$$

and the differentiation is performed in the LR system, at constant pressure P and molality m . In these relations, R is the gas constant, T is temperature, ν is the stoichiometric number of the salt, and ϕ^{LR} and γ^{LR} are the LR osmotic and mean molal activity coefficients of the salt, respectively.

One obtains from the latter two relations,

$$L_\phi = \nu N_A \frac{\partial(1 - \phi^{LR} + \ln \gamma^{LR})}{\partial \beta} \Big|_{P,m} \quad (4)$$

where N_A is Avogadro's number, $(\phi^{LR} - 1)$ represents the excess LR osmotic coefficient, and $\beta = 1/k_B T$ with k_B is the Boltzmann constant ($k_B = R/N_A$).

It is shown now how this expression for L_ϕ can be expressed in terms of quantities at the McMillan-Mayer (MM) level, at which the continuum solvent model is developed. Hereafter, we consider a binary solution of a strong salt in water.

First, the LR activity and osmotic coefficients are expressed as functions of their MM counterparts according to Eqs. (5) and (6) below [29, 30],

$$\ln \gamma^{LR} = \ln \gamma^{MM} - C_t V_\pm \phi^{MM} + \ln \left(\frac{V_w^0}{V} \right) \quad (5)$$

with γ^{MM} the mean salt activity coefficient on molar scale at MM level, $C_t = \nu C$ the total solute concentration (with C the salt concentration), V_\pm the mean solute partial molal volume of solution, ϕ^{MM} the MM osmotic coefficient, V_w^0 the specific volume of pure water ($= 1/d_0$, with d_0 its density), and V the specific volume of solution (volume per kg of water). In Eq. (5), the last term on the r.h.s. corresponds to the conversion of γ^{MM} to the LR activity coefficient on molar scale. The second term on the r.h.s. of this equation corresponds to the MM-to-LR conversion [30].

The MM-to-LR conversion of the osmotic coefficient gives,

$$\phi^{LR} = \phi^{MM} (1 - C_t V_\pm) \quad (6)$$

By using Eqs. (5) and (6) in Eq. (4) one finds after simplification,

$$L_\phi = \nu N_A \frac{\partial}{\partial \beta} \left[1 - \phi^{MM} + \ln \gamma^{MM} + \ln \left(\frac{V_w^0}{V} \right) \right] \Big|_{P,m} \quad (7)$$

This expression may be further simplified by using the relation [33],

$$1 - \phi^{MM} + \ln \gamma^{MM} = \beta A^{MM} / \rho_t \quad (8)$$

in which A^{MM} is the excess Helmholtz energy per unit volume at the MM level of the model, and ρ_t is the total number density of solute,

$$\rho_t = N_A C_t = N_A \nu C \quad (9)$$

with C expressed in SI units (mol m^{-3}). One arrives at,

$$L_\phi = \nu N_A \frac{\partial}{\partial \beta} \left[\frac{\beta A^{MM}}{\rho_t} + \ln \left(\frac{V_w^0}{V} \right) \right] \Big|_{P,m} \quad (10)$$

Care must be exercised in this differentiation at constant P and m . Ref. 28 gives us an indication of how to do this properly. Since the pressure is constant when T is varied, one may use Eqs. (8) and (13) of this latter reference to write,

$$\frac{\partial(\beta A^{MM}/\rho_t)}{\partial \beta} \Big|_{P,m} = \frac{\partial(\beta A^{MM}/\rho_t)}{\partial \beta} \Big|_{\rho_t} + \frac{\partial(\beta A^{MM}/\rho_t)}{\partial(1/\rho_t)} \frac{\partial(1/\rho_t)}{\partial \beta} \Big|_m \quad (11)$$

where the constant pressure has been omitted for convenience on the r.h.s. of this relation.

In the first term, one may use the fundamental thermodynamic relation: $\partial(\beta A^{MM})/\partial \beta = U^{MM}$, where U^{MM} is the excess internal energy per unit volume of the system at MM level. In the second term, one may utilize Eq. (10) of Ref. 33 from which one gets,

$$\frac{\partial(\beta A^{MM}/\rho_t)}{\partial(1/\rho_t)} = \rho_t (1 - \phi^{MM}) \quad (12)$$

Moreover, by virtue of Eq. (9) and the relation $C = m/V$, one has

$$\frac{\partial(1/\rho_t)}{\partial \beta} \Big|_m = \frac{1}{\nu m N_A} \frac{\partial V}{\partial \beta} \Big|_m \quad (13)$$

By combining these relations, Eq. (11) thus becomes,

$$\frac{\partial(\beta A^{MM}/\rho_t)}{\partial \beta} \Big|_{P,m} = \frac{U^{MM}}{\rho_t} + (1 - \phi^{MM}) \frac{\partial \ln V}{\partial \beta} \Big|_m \quad (14)$$

Finally, it stems from Eqs. (10) and (14), and after simplification, that,

$$L_\phi = \frac{U^{MM}}{C} + \nu R T^2 \left(\phi^{MM} \frac{\partial \ln V}{\partial T} \Big|_m - \frac{\partial \ln V_w^0}{\partial T} \right) \quad (15)$$

with C expressed in mol m^{-3} .

This relation could also have been obtained by using Eq. (15) of Ref. 28 and making the approximation that the solution is incompressible (which is already assumed in Eqs. (5) and (6) for the MM-to-LR conversion [29, 30]). This latter approximation then entails some simplifications in the equations [30] that finally lead to Eq. (14).

The next section is devoted to an examination of the internal energy U^{MM} that appears in Eq. (14).

2.2. Total internal energy in models with continuum solvent

2.2.1. A basic relation

As first pointed out by Rushbrooke [34] in 1940, the total internal energy of a system, in which the energy levels of the accessible states explicitly depend upon the temperature, is *not* given by the internal energy expressed classically in models in which the energy levels are temperature-independent or assumed to be so. The fundamental reason for this is that the probability of a state of energy $E(T)$ is not given by a Boltzmann factor of the form $\exp[-E(T)/k_B T]$. Nonetheless, Rushbrooke indicated the way the two are connected [34].

This is illustrated now in the case of an ionic solution modeled as a collection of simple spherical ions distributed in an implicit solvent mimicking the properties of water.

In continuum solvent models like the DH theory or the MSA, it is often assumed that the electrostatic interaction potential between ions i and j carrying charges q_i and q_j at their center, and separated by a distance r between their centers, is expressed as,

$$u_{ij}^{el}(r) = \frac{1}{4\pi\epsilon_0} \frac{1}{\epsilon(T)} \frac{q_i q_j}{r} \quad (16)$$

so having the same form as the *direct* Coulomb potential (in a vacuum), $u_{ij}^{el(0)}(r) = (1/4\pi\epsilon_0) q_i q_j / r$. In these equations, ϵ_0 is the permittivity of a vacuum and $\epsilon(T)$ is the relative permittivity of the solution, which is a function of temperature.

Following Rushbrooke [34], the interaction potential of ions i and j to be taken in thermodynamic studies of an electrolyte is,

$$\begin{aligned} w_{ij}(r) &= \frac{\partial[\beta u_{ij}(r)]}{\partial\beta} \\ &= u_{ij}(r) + \beta \frac{\partial u_{ij}(r)}{\partial\beta} \end{aligned} \quad (17)$$

Generally, u_{ij} is the sum of the electrostatic term of Eq. (16) and a contribution corresponding to hard core repulsion [see Eq. (20)]. It varies with temperature because, conceptually, it can be viewed as resulting from an *average* of the potential of the system upon the states (coordinates) of the solvent. Eq. (17) expresses that this property introduces an additional term to $u_{ij}(r)$.

As mentioned by Rasaiah and Friedman [35], the total electrostatic internal energy of an electrolyte solution is then given by,

$$U^{MM} = \frac{1}{2} \sum_{i,j} \rho_i \rho_j \int_0^\infty g_{ij}(r) \frac{\partial[\beta u_{ij}(r)]}{\partial\beta} 4\pi r^2 dr \quad (18)$$

where ρ_i is the number density of ions of type i , and g_{ij} is the radial distribution function (RDF) for ions i and j . Eq. (18) replaces the relation that is commonly utilized in the literature, which involves simply an integral of u_{ij} over r when u_{ij} does not depend explicitly on the temperature.

2.2.2. Internal energy

In analytic models with implicit continuum solvent like the MSA, ions are modeled as charged hard spheres. Beside the variation of the permittivity with T , another parameter expected to be temperature-dependent is the diameter of the ions. This dependence originates from the variation of ion-water and water-water interactions with temperature, which in turn modify the effective ion-ion interactions. Assuming a varying ion-ion least distance of approach, or of the ion sizes, is a convenient way of modeling this modification.

The full interaction potential is written as,

$$u_{ij} = u_{ij}^{HS} + u_{ij}^{el} \quad (19)$$

in which the hard sphere (HS) potential u_{ij}^{HS} is a function of the minimum distance of approach between ions i and j . One has,

$$\begin{cases} u_{ij}^{HS}(r) = +\infty, & \text{for } r < \sigma_{ij} \\ u_{ij}^{HS}(r) = 0, & \text{for } r \geq \sigma_{ij} \end{cases} \quad (20)$$

where σ_{ij} is the minimum approach distance of ions of type i and j . It will be assumed that

$$\sigma_{ij} = (\sigma_i + \sigma_j)/2 \quad (21)$$

with σ_k the diameter of an ion of type k .

The total excess internal energy of the system (ions plus solvent), U^{MM} , is given by Eqs. (18) and (19). Using Eq. (17) and the chain rule one can write that,

$$\frac{\partial(\beta u_{ij})}{\partial\beta} = u_{ij} + \frac{\partial(\beta u_{ij})}{\partial\varepsilon^{-1}} \frac{\partial\varepsilon^{-1}}{\partial\beta} + \frac{\partial(\beta u_{ij})}{\partial\sigma_{ij}} \frac{\partial\sigma_{ij}}{\partial\beta} \quad (22)$$

from which one gets,

$$U^{MM} = U_0 + U_\varepsilon + U_\sigma \quad (23)$$

where

$$U_0 = 2\pi \sum_{i,j} \rho_i \rho_j \int_0^\infty g_{ij}(r) u_{ij}(r) r^2 dr \quad (24)$$

is the usual internal energy in models at MM level when the permittivity and the ion sizes are constant versus T , and

$$U_\varepsilon = 2\pi \sum_{i,j} \rho_i \rho_j \frac{\partial\varepsilon^{-1}}{\partial\beta} \int_0^\infty g_{ij}(r) \frac{\partial[\beta u_{ij}(r)]}{\partial\varepsilon^{-1}} r^2 dr \quad (25)$$

$$U_\sigma = 2\pi \sum_{i,j} \rho_i \rho_j \frac{\partial\sigma_{ij}}{\partial\beta} \int_0^\infty g_{ij}(r) \frac{\partial[\beta u_{ij}(r)]}{\partial\sigma_{ij}} r^2 dr \quad (26)$$

In the equation for U_ε , it is clear from Eqs. (16) and (19) that

$$\frac{\partial u_{ij}}{\partial\varepsilon^{-1}} = \varepsilon u_{ij} \quad (27)$$

which yields by virtue of Eqs. (24) and (25) the well-known additional Bjerrum contribution [15] arising from the change of the dielectric properties of the solvent,

$$U_\varepsilon = \beta\varepsilon \frac{\partial\varepsilon^{-1}}{\partial\beta} U_0 \quad (28)$$

A workable expression for U_σ is less straightforward to obtain. The first step is to write,

$$\frac{\partial(\beta u_{ij})}{\partial\sigma_{ij}} = -\exp(\beta u_{ij}) \frac{\partial[\exp(-\beta u_{ij})]}{\partial\sigma_{ij}} \quad (29)$$

Now, using Eqs. (19) and (20), one readily finds that,

$$\exp[-\beta u_{ij}(r)] = \exp[-\beta u_{ij}^{el}(r)] H(r - \sigma_{ij}) \quad (30)$$

in which H is the Heaviside step function (distribution): $H(x) = 0$ for $x < 0$ and $H(x) = 1$ for $x > 0$. One therefore obtains,

$$\frac{\partial[\exp(-\beta u_{ij}(r))]}{\partial \sigma_{ij}} = -\exp[-\beta u_{ij}^{el}(r)] \delta(r - \sigma_{ij}) \quad (31)$$

with δ the Dirac delta function (distribution): $\delta(0) = +\infty$ and $\delta(x) = 0$ for $x \neq 0$.

By employing Eqs. (29) and (31), one gets,

$$\begin{aligned} \int_0^\infty g_{ij}(r) \frac{\partial[\beta u_{ij}(r)]}{\partial \sigma_{ij}} r^2 dr &= \int_0^\infty \{g_{ij}(r) \exp[\beta u_{ij}(r)]\} \exp[-\beta u_{ij}^{el}(r)] \delta(r - \sigma_{ij}) r^2 dr \\ &= \int_0^\infty y_{ij}(r) \exp[-\beta u_{ij}^{el}(r)] \delta(r - \sigma_{ij}) r^2 dr \\ &= \sigma_{ij}^2 g_{ij}^c \end{aligned} \quad (32)$$

in which $y_{ij} = g_{ij} \exp(\beta u_{ij})$ is the cavity distribution function, and $g_{ij}^c = g_{ij}(\sigma_{ij})$ is the RDF at contact of ions i and j . The function y_{ij} has been introduced because it has the remarkable property of being a continuous function of r [36]. Then the last equality in this equation is obtained by using this property at $r = \sigma_{ij}^+$ where $u_{ij} = u_{ij}^{el}$.

Insertion of this result in Eq. (26) gives the following relation,

$$U_\sigma = 2\pi \sum_{i,j} \rho_i \rho_j \sigma_{ij}^2 g_{ij}^c \frac{\partial \sigma_{ij}}{\partial \beta} \quad (33)$$

This expression can be simplified by using Eq. (21), which yields,

$$U_\sigma = 2\pi \sum_i \rho_i \omega_i \frac{\partial \sigma_i}{\partial \beta} \quad (34)$$

with

$$\omega_i = \sum_k \rho_k \sigma_{ik}^2 g_{ik}^c \quad (35)$$

We note in passing that, because $U^{MM} = \partial(\beta A^{MM})/\partial \beta$, relation (34) also means that $(\partial \beta A^{MM}/\partial \sigma_i) = 2\pi \rho_i \omega_i$, which entails that the following relation must be fulfilled,

$$\rho_i \frac{\partial \omega_i}{\partial \sigma_j} = \rho_j \frac{\partial \omega_j}{\partial \sigma_i} \quad (36)$$

This equation seems to be a new relation, imposing a condition on the contact RDF's of the ions when the latter are modeled as hard spheres. It was found that the result from the scaled-particle theory for a fluid of hard spheres [37] satisfies this relation. This is not so for the RDF derived from the work by Carnahan and Starling [37] or the Percus-Yevick equation [38] for hard spheres, or the MSA RDF for ions [39].

If we now specialize to the case of a binary solution of a strong 1:1 salt (salts in which one ion is multivalent generally exhibit ion pairing in water), then one has $\nu = 2$ and $\rho_+ = \rho_- = \rho$, in which $+$ and $-$ designate the cation and anion, respectively.

In the restricted case where the cation and anion have the same diameter, $\sigma_+ = \sigma_- = \sigma$, one gets from Eq. (34),

$$U_\sigma = 4\pi\rho^2\sigma^2 (g_{++}^c + g_{+-}^c) \frac{\partial\sigma}{\partial\beta} \quad (37)$$

because $g_{--}^c = g_{++}^c$ in that case.

In the unrestricted case where the cation and anion have arbitrary diameters, and only the cation size σ_+ varies with temperature [40, 41] (and σ_- remains equal to its crystallographic diameter), one obtains using Eq. (21),

$$U_\sigma = 2\pi\rho^2 (\sigma_+^2 g_{++}^c + \sigma_{+-}^2 g_{+-}^c) \frac{\partial\sigma_+}{\partial\beta} \quad (38)$$

Finally, to summarize, the dilution enthalpy resulting from Eqs. (15) and (23) may be expressed as,

$$L_\phi = \frac{U_0}{C} + \frac{U_\varepsilon}{C} + \frac{U_\sigma}{C} + \nu RT^2 \left(\phi^{MM} \frac{\partial \ln V}{\partial T} \Big|_m - \frac{\partial \ln V_w^0}{\partial T} \right) \quad (39)$$

in which U_0 , U_ε , and U_σ , are given by Eqs. (A.1) ($U_0 = U^{MSA}$ when the MSA is used), (28) and (34), respectively.

3. Results and discussion

The above analysis is now applied to the modeling of dilution enthalpy data within the MSA, for aqueous solutions of lithium chloride at temperatures ranging from 25°C to 100°C, and 0 to 6 mol kg⁻¹.

This salt was chosen for the following reasons. It is a strong salt at 25°C [42] and the lithium ion is the most hydrated monovalent metal cation [43]. In this work, it was assumed that LiCl is a strong salt in water up to 100°C, with the lithium ion keeping a firmly bound hydration sheath in this temperature range.

The dilution enthalpy data were taken from works by Wu and Young [13] (at 25°C only) and Gibbard and Scatchard [44]. The data of Wu and Young resulted from calorimetric measurements. Those of Gibbard and Scatchard were obtained from calorimetric measurements at 25°C [5] and from vapor-liquid equilibrium experiments (yielding γ^{LR} and ϕ^{LR} values from which dilution enthalpy data were obtained by employing the same methodology as in this work). In passing, it is noted that data at 0°C were also given in Ref. [44] (but not mentioned in the title of the publication); they were not considered in the present study because, surprisingly, the origin of these data was not specified and remains unknown; moreover, it was observed that these data were not well described by the treatment developed hereafter.

The method used in the present investigation was, first, to optimize a description of data for activity and osmotic coefficients within the MSA (a model with continuum implicit solvent at MM level), and then, by using the values of the adjusted parameters, to check that the values for the dilution enthalpies obtained from Eq. (15) are in agreement with published data.

3.1. Activity and osmotic coefficients

Thus, in the first place, deviations from ideality for LiCl aqueous solutions were described at temperatures going from 25°C to 100°C. The data for γ^{LR} and ϕ^{LR} were retrieved from the same source as for dilution enthalpies [44], and fitted using the mean spherical approximation (MSA) [20, 33, 39, 40, 45]. The MSA expressions for γ^{MM} and ϕ^{MM} , together with that for the internal energy, are given in Appendix A.

The MM-to-LR conversion has a strong effect on activity and osmotic coefficients at high ionic strength [30]. In the case of LiCl at 5 molar (~ 6 molal), it is found that it produces a $\sim 33\%$ decrease in γ and a $\sim 10\%$ decrease in ϕ . These changes are nearly constant in the range of 25°C to 100°C .

Two types of MSA models were employed, namely the restricted case in which the sizes of cation and anion are equal and vary with C and T ; and the unrestricted case in which the two ions have different diameters and only the diameter of the cation varies with C and T [33, 40]. In the latter case, the anion size was assumed to be constant vs. temperature, equal to its Pauling crystallographic diameter. In the two versions, the relative solution permittivity was assumed to vary with C and T .

Following previous work [33, 40, 41], it was supposed that the ion size and the inverse of the permittivity vary linearly with the salt concentration as,

$$\sigma = \sigma^{(0)}(T) + \sigma^{(1)}(T) C \quad \text{and} \quad \varepsilon^{-1} = \varepsilon_w(T)^{-1} [1 + \alpha(T) C] \quad (40)$$

where σ stands for the diameter of cation and anion in the restricted case, or for σ_+ in the unrestricted case, and ε_w is the dielectric constant of water. The parameter $\sigma^{(0)}$ is the diameter of the ion at infinite dilution, and $\sigma^{(1)}$ and α stand for the rates of variation of σ and ε^{-1} with concentration. The rationale behind Eq. (40) is that σ does not vary too much with C , this equation being then a first-order Taylor expansion of σ vs. C , and ε has the same type of variation as the experimental permittivity [46]. Because the degree of ion hydration and the amount of free water are expected to drop with salt concentration, one should have $\sigma^{(1)} < 0$ and $\alpha > 0$, so that σ and ε decrease with C .

These two relations were introduced originally on the assumption that the ion size varies relatively little on the interval of concentration, and on the observation that the inverse of the experimental relative permittivity of solution, ε_{sol}^{-1} , varies approximately linearly with concentration [46]. Let us notice however that ε_{sol} is likely to differ from the static ε needed in thermodynamic models [47–50].

In Eq. (40), $\sigma^{(0)}(T)$, $\sigma^{(1)}(T)$, and $\alpha(T)$ were (empirically) taken as polynomial functions of the relative temperature difference, $(T - T_0)/T_0$, where $T_0 = 298.15$ K ($= 25^\circ\text{C}$),

$$f(T) = f_0 + f_1 \frac{T - T_0}{T_0} + f_2 \left(\frac{T - T_0}{T_0} \right)^2 + \dots \quad (41)$$

in which $f_0 = f(T_0)$, and $f = \sigma^{(0)}$ (or $\sigma_+^{(0)}$), $\sigma^{(1)}$ (or $\sigma_+^{(1)}$), or α . In this work, polynomials of the second degree were used for a fit of the data for LiCl solutions. Using polynomials of the third degree did not improve appreciably the results for the dilution enthalpies.

The present description therefore involves 9 parameters. The model employed in the original work of Gibbard and Scatchard involved 25 parameters [44]. It is well known that, in general, a rather large number of parameters is required in any model to describe first-order derivative thermodynamic properties as a function of concentration and temperature.

In Eq. (40), the dielectric constant of water, ε_w , is known with accuracy from experiment as a function of temperature between 0°C and 100°C [51]. A formula was proposed in the latter work as,

$$\log_{10} \varepsilon_w = 1.94315 - 0.0019720 t \quad (42)$$

where t is the temperature in degrees Celsius.

The specific volume V was obtained from the general relation,

$$V = (1 + mM)/d \quad (43)$$

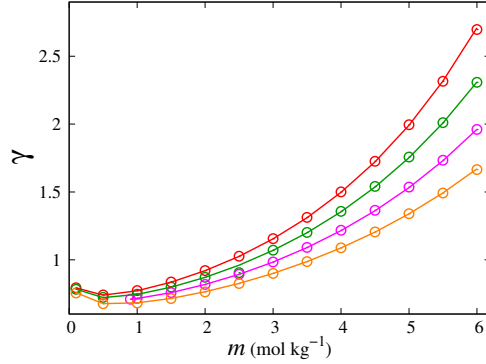


Figure 1: Fit of mean salt activity coefficient of LiCl in aqueous solutions up to 6 mol kg⁻¹ at temperatures of, from top to bottom: 25°C, 50°C, 75°C, 100°C. Solid lines: results of fit. The curves for the restricted and unrestricted case cannot be distinguished from each other.

Table 1: Parameter values obtained from fit of γ^{LR} and ϕ^{LR} in the restricted case ($\sigma_+ = \sigma_-$)

$\sigma_0^{(0)}$ (Å)	$\sigma_1^{(0)}$ (Å)	$\sigma_2^{(0)}$ (Å)	$10^2\sigma_0^{(1)}$ (Å mol ⁻¹ L)	$10^2\sigma_1^{(1)}$ (Å mol ⁻¹ L)	$10^2\sigma_2^{(1)}$ (Å mol ⁻¹ L)	$10^2\alpha_0$ (mol ⁻¹ L)	$10^2\alpha_1$ (mol ⁻¹ L)	$10^2\alpha_2$ (mol ⁻¹ L)
4.301	-0.2640	-0.9161	-3.444	-0.7586	5.045	7.923	-2.053	-13.01

in which M is the salt molar mass and d is the solution density. The latter was computed using a formula of the form $d = d_w + d_1C + d_2C^{3/2}$, where d_w , d_1 , and d_2 are quadratic polynomials of the temperature given in Ref. 52. The derivative of $\ln V$ w.r.t. T at constant m in Eq. (15) was computed using Eq. (43), which yields the relation,

$$\left. \frac{\partial \ln V}{\partial T} \right|_m = - \left. \frac{(\partial d / \partial T)}{d - C \partial d / \partial C} \right|_C \quad (44)$$

The derivative $\partial \ln V_w^0 / \partial T$ is obtained by taking $C = 0$ in the latter equation.

In Eqs. (5) and (6), the mean solute partial molal volume of solution, V_{\pm} , was computed using the equation [30],

$$V_{\pm} = \frac{1}{2} \frac{M - \partial d / \partial C}{d - C \partial d / \partial C} \quad (45)$$

The experimental LR mean salt activity and osmotic coefficients were fitted at the same time. The objective function was the sum of the absolute relative deviations of the calculated γ^{LR} and ϕ^{LR} as compared to the experimental. All the data up to 6 mol kg⁻¹ were included in the fit, except for the γ^{LR} values from 0.1 to 0.8 mol kg⁻¹ at 75°C, which are erroneously equal to those for ϕ^{LR} in Ref. 44 (the data for ϕ^{LR} were not included either in the fit).

The results for the fit of γ^{LR} and ϕ^{LR} are shown in Figures 1 and 2, respectively. The adjusted parameter values are collected in Table 1 in the restricted case (equisized cation and anion). The average absolute relative deviations (AARD's) of fit were of 0.06% for γ^{LR} and 0.05% for ϕ^{LR} . The results in the unrestricted case are shown in Table 2. The AARD's of fit were of 0.05% for γ^{LR} and 0.04% for ϕ^{LR} , which is a little better than in the restricted case.

The variation of $\sigma^{(0)}$, $\sigma^{(1)}$, and α in the restricted and unrestricted cases is plotted in Figures 3-5. It is seen in Fig. 3 that the diameter at infinite dilution, $\sigma^{(0)}$ or $\sigma_+^{(0)}$, decreases with T

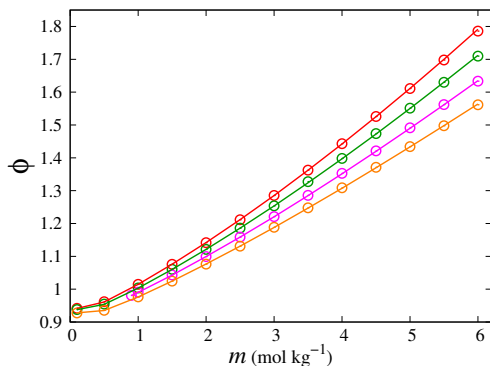


Figure 2: Fit of osmotic coefficient for LiCl aqueous solutions up to 6 mol kg⁻¹ at temperatures of, from top to bottom: 25°C, 50°C, 75°C, 100°C. Solid lines: results of fit. The curves for the restricted and unrestricted case cannot be distinguished from each other.

Table 2: Same as Table 1 in the unrestricted case (varying σ_+ , and $\sigma_- = 3.62 \text{ \AA}$)

$\sigma_{+,0}^{(0)}$ (\AA)	$\sigma_{+,1}^{(0)}$ (\AA)	$\sigma_{+,2}^{(0)}$ (\AA)	$10^2 \sigma_{+,0}^{(1)}$ ($\text{\AA mol}^{-1} \text{ L}$)	$10^2 \sigma_{+,1}^{(1)}$ ($\text{\AA mol}^{-1} \text{ L}$)	$10^2 \sigma_{+,2}^{(1)}$ ($\text{\AA mol}^{-1} \text{ L}$)	$10^2 \alpha_0$ ($\text{mol}^{-1} \text{ L}$)	$10^2 \alpha_1$ ($\text{mol}^{-1} \text{ L}$)	$10^2 \alpha_2$ ($\text{mol}^{-1} \text{ L}$)
5.000	-0.6365	-1.483	-6.920	-0.4819	8.042	9.170	-5.305	-9.280

in the two cases. This behavior was expected considering that thermal agitation may favor a loosening of the water molecules around a hydrated ion, and consequently a shrinking of the hydration shell. The drop of $\sigma^{(0)}$ or $\sigma_+^{(0)}$ with temperature might also be a consequence of the breaking down of the tetrahedral structure of water when temperature is increased [53]. This disintegration of the H-bond network is expected to modify the cation-anion potential of mean force, leading to a drop of the minimum distance of approach of these ions. By virtue of Eq. (21) for σ_{+-} , this will produce a reduction of the value of $\sigma^{(0)}$ or $\sigma_+^{(0)}$ in the model.

Figure 4 shows that the rate of *decrease* of the ion diameter, expressed by $-\sigma^{(1)}$, first increases slightly with T and then decreases in the two cases. This initial increase is very small in the unrestricted case which is the more realistic one, with a hydrated cation and an essentially unhydrated anion (the restricted case has less physical meaning). The slight initial rise of $-\sigma^{(1)}$ is difficult to interpret. It is likely due to a small artifact of the model. Nonetheless, the predominantly decreasing profile of $-\sigma^{(1)}$ with T in that case is in keeping with an expected propensity of an ion to lose water molecules less easily when the ion becomes progressively less hydrated. Likewise, as expected, it is observed that the rate of decrease of the permittivity, α , drops with T together with the dielectric constant of water, ϵ_w .

3.2. Results for the dilution enthalpies of LiCl solutions

The expression for the apparent relative molal enthalpy, L_ϕ , is given by Eq. (15) together with the relation for U^{MM} provided by Eq. (23).

The contribution, U_σ , expressed in Eq. (34), involves the RDF at contact, g_{ij}^c . The MSA value of this RDF [39] is known to be quite inaccurate [54], even at low salt concentration where the like RDF can be negative [20]. In some cases, the MSA contact RDF for unlike ions is too small by a factor of the order of 2. Moreover, it does not fulfill Eq. (36). The MSA RDF

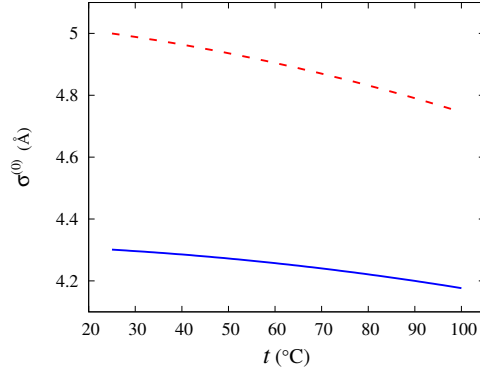


Figure 3: Ion diameters at infinite dilution as a function of temperature [see Eq. (40)]. Solid line: $\sigma^{(0)}$ (restricted case); dashed line: $\sigma_+^{(0)}$ (unrestricted case).

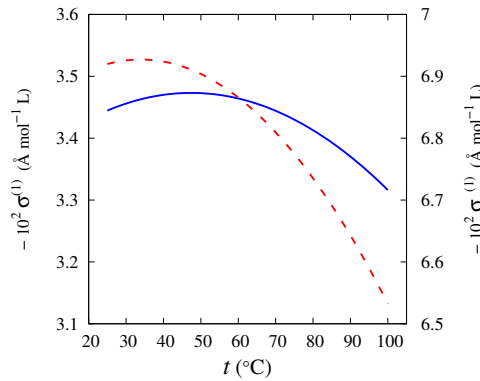


Figure 4: Parameter for the variation of ion size with concentration, as a function of temperature [see Eq. (40)]. Solid line: $-\sigma^{(1)}$, restricted case (left scale); dashed line: $-\sigma_+^{(1)}$, unrestricted case (right scale).

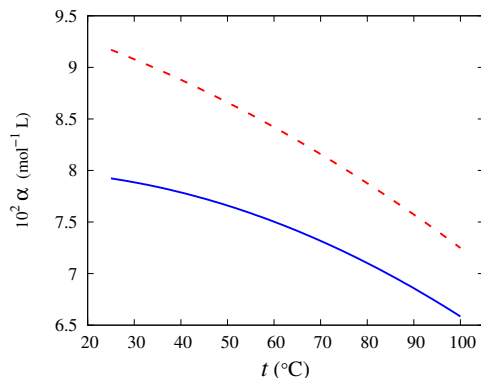


Figure 5: Parameter α for the variation of permittivity with concentration, as a function of temperature [see Eq. (40)]. Solid line: restricted case; dashed line: unrestricted case.

therefore cannot be used for the prediction of dilution enthalpies.

3.2.1. Restricted case: $\sigma_+ = \sigma_- = \sigma$

Nevertheless, a theoretical result is available in the literature in the restricted case (equisized cation and anion) for a symmetric electrolyte ($\rho_+ = \rho_-$) [54]. The equations for the RDF are outlined in Appendix B. They were utilized in Eq. (37).

The result for the dilution enthalpies of LiCl aqueous solutions is plotted in Figure 6 in the restricted case of the MSA. The agreement with the data of Refs. 13 and 44 is very good for the latter and fair for the former. The overall average absolute relative deviation (AARD) for these data is $\sim 2.6\%$; it is of $\sim 1.6\%$ for the data of Gibbard and Scatchard [44], and of $\sim 6\%$ for those of Wu and Young [13]. The reason for this difference is that the L_ϕ values of the first reference were computed from a fit of the activity and osmotic coefficients data, as in the present work, while the L_ϕ values of the second one were measured experimentally, and are not fully consistent with the data of Gibbard and Scatchard.

It may be seen in Fig. 6 that the data exhibit an inflection point as a function of m . A calculation of the derivatives of L_ϕ shows that the location of this point increases with temperature, from $m \simeq 2 \text{ mol kg}^{-1}$ at 25°C to $m \simeq 3.4 \text{ mol kg}^{-1}$ at 100°C . The four contributions to L_ϕ in Eq. (39) at 25°C are plotted in Figure 7. It is seen in the left panel that the dominant contributions, U_0/C and U_ε/C , corresponding to electrostatic interactions and to the temperature variation of the dielectric properties of the solvent, respectively, are of opposite sign. Being of comparable orders of magnitude, they partly compensate each other. The right panel shows that their sum is positive, and larger than U_σ/C below 4.6 mol kg^{-1} , and smaller above. It reaches a value of $\sim 1660 \text{ J mol}^{-1}$ at 6 mol kg^{-1} where $U_\sigma/C \sim 2200 \text{ J mol}^{-1}$ (curve 3 in Figure 7). The latter increases rapidly with C . In this breakdown, U_σ/C and, to a lesser extent, the contribution to L_ϕ arising from the variation of the solution density with concentration [the last term in brackets in Eq. (39)], are responsible for the inflection point observed in L_ϕ as a function of m (their second derivative w.r.t. C or m is positive). Thus, U_σ/C constitutes a contribution of significant magnitude to L_ϕ .

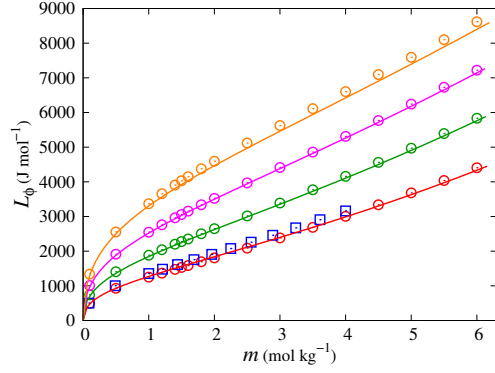


Figure 6: Dilution enthalpies for LiCl aqueous solutions up to 6 mol kg^{-1} within the restricted MSA. For each curve, the temperatures are, from bottom to top : 25°C , 50°C , 75°C , 100°C . Symbols: (\odot) Data of Gibbard and Scatchard [44]; (\square) data of Wu and Young at 25°C [13]. Solid lines: calculated L_ϕ values.

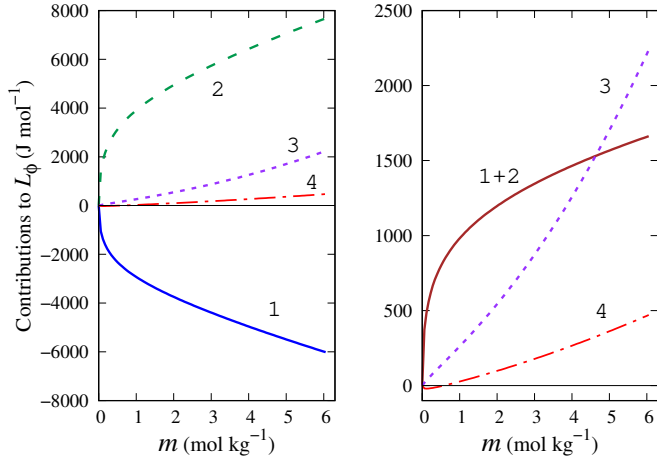


Figure 7: Contributions to the dilution enthalpies in the r.h.s. of Eq. (39) for LiCl aqueous solutions at 25°C within the restricted MSA. Left panel: (1) U_0/C ; (2) U_ε/C ; (3) U_σ/C ; (4) last term in brackets in Eq. (39). Right panel: (1+2) $(U_0 + U_\varepsilon)/C$; (3) and (4) unchanged.

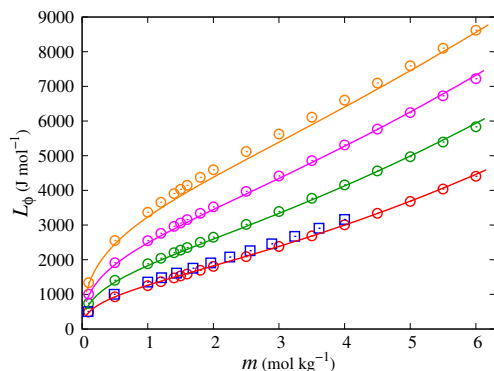


Figure 8: Same as for Figure 6 within the *unrestricted* MSA.

3.2.2. Unrestricted case: $\sigma_+ \neq \sigma_-$

No equation for the RDF's at contact is available for ions of different sizes. Only an approximate formula may be employed in this case.

In this work, this was done by looking for a mean ion diameter to be used in the equations of Appendix B for g_{++}^c and g_{+-}^c , and then in Eq. (38) for U_σ . A first glance at this equation indicates that a candidate could be the mean of σ_+ and σ_{+-} that are involved in the expression of U_σ , that is,

$$\bar{\sigma} = \frac{3}{4}\sigma_+ + \frac{1}{4}\sigma_- \quad (46)$$

It was found numerically that the optimum diameter for the description of L_ϕ for LiCl solutions at all temperatures between 25°C and 100°C is indeed close to this $\bar{\sigma}$, namely $\sigma^{opt} \simeq (1 - 0.244)\sigma_+ + 0.244\sigma_-$. The mean diameter $\bar{\sigma}$ was employed in Eq. (38) for U_σ , by assuming that g_{++}^c and g_{+-}^c are given by Eqs. (B.8) and (B.10) in which $\bar{\sigma}$ is used for σ .

The result for the dilution enthalpies of LiCl aqueous solutions is plotted in Figure 8 in the unrestricted case of the MSA. It is just slightly less good than in the preceding section within the restricted MSA. The overall AARD is now $\sim 3.6\%$ as compared to $\sim 2.6\%$ before.

It was found that the result for L_ϕ below 2 mol kg⁻¹ is weakly sensitive to the precise value taken for σ in g_{++}^c and g_{+-}^c of Eqs. (B.8) and (B.10). It becomes more and more sensitive as C is increased.

4. Conclusion

In this work, it has been shown how to calculate dilution enthalpies of aqueous solutions of strong salts from a description with implicit solvent. A compact expression has been obtained for this quantity, that involves the internal energy of the solution at MM level.

The MSA has been used here for an application because it is a consistent and accurate model for aqueous solutions of monovalent salts, in particular as compared to the DH theory [55]. The expression for the dilution enthalpy has been validated in the case of LiCl aqueous solutions up to 6 mol kg⁻¹ in the 25°C-100°C temperature range. The restricted and unrestricted versions of the MSA have been utilized.

The most convenient and apparently accurate one is the restricted MSA because an analytic expression for the RDF at contact is available in the literature, not when the cation and anion

have different sizes. However, an approximate way of computing the corresponding contribution to the dilution enthalpy (U_σ) has been proposed to circumvent this issue, but its general validity will have to be confirmed subsequently.

In future work, the case of aqueous solutions of other monovalent salts will be studied. The case of higher valence salts would also deserve due attention. However, when the temperature becomes sufficiently high, the two types of salts will require introducing ion pairing in the model, which will make the description more challenging to develop. It will also be attempted to obtain an expression for the heat capacity in the framework of implicit-solvent models. Computation of this second-order derivative property will require a very accurate description of the thermodynamic properties of the solutions.

Declaration of Competing Interest

The author declares that he has no competing financial interests or personal relationships that could have influenced the work reported in this paper.

Appendix A. Basic MSA equations

The excess electrostatic energy per unit volume, U_0 , of Eqs. (23) and (24) was calculated within the MSA: $U_0 = U^{MSA}$. Its expression is given by [33],

$$\beta U^{MSA} = -\lambda \sum_k \rho_k z_k N_k \quad (\text{A.1})$$

where

$$\lambda = \beta e^2 / (4\pi \epsilon_0 \epsilon_w) \quad (\text{A.2})$$

e is the elementary charge, and z_k is the valence of ions of type k ,

$$N_k = -\frac{\Gamma z_k + \eta \sigma_k}{1 + \Gamma \sigma_k} \quad (\text{A.3})$$

$$\eta = \frac{1}{\Omega} \frac{\pi}{2\Delta} \sum_k \frac{\rho_k \sigma_k z_k}{1 + \Gamma \sigma_k} \quad \Omega = 1 + \frac{\pi}{2\Delta} \sum_k \frac{\rho_k \sigma_k^3}{1 + \Gamma \sigma_k} \quad (\text{A.4})$$

where Δ is the volume fraction of free space (not occupied by solute particles), $\Delta = 1 - (\pi/6) \sum_k \rho_k \sigma_k^3$, and Γ is the MSA screening parameter which satisfies the equation,

$$\Gamma^2 = \pi \lambda \sum_k \rho_k [(z_k - \eta \sigma_k^2) / (1 + \Gamma \sigma_k)]^2 \quad (\text{A.5})$$

Its value can be easily determined numerically by rewriting Eq. (A.5) as $\Gamma = f(\Gamma)$ and using the iterative procedure $\Gamma_{n+1} = f(\Gamma_n)$ with, e.g., $\Gamma_0 = \kappa/2$ (where κ is the Debye screening parameter), which converges in a few steps.

The mean salt activity and osmotic coefficients at MM level are expressed as [33],

$$\ln \gamma^{MM} = \ln \gamma^{HS} + \ln \gamma^{MSA} \quad \text{and} \quad \phi^{MM} = 1 + \phi^{HS} + \phi^{MSA} \quad (\text{A.6})$$

One has,

$$\ln \gamma^{MSA} = \frac{\beta U^{MSA}}{\rho_t} - \lambda \frac{2\eta^2}{\pi \rho_t} + \frac{1}{\rho_t} \sum_k \rho_k q_k D(\sigma_k) + \frac{\beta U^{MSA}}{\rho_t} \epsilon D(\epsilon^{-1}) \quad (\text{A.7})$$

and

$$\phi^{MSA} = -\frac{\Gamma^3}{3\pi\rho_t} - \lambda\frac{2\eta^2}{\pi\rho_t} + \frac{1}{\rho_t} \sum_k \rho_k q_k D(\sigma_k) + \frac{\beta U^{MSA}}{\rho_t} \varepsilon D(\varepsilon^{-1}) \quad (\text{A.8})$$

in which,

$$q_k = \lambda \left[\frac{\Gamma^2 z_k^2}{(1 + \Gamma\sigma_k)^2} + \eta \frac{\eta\sigma_k^2(2 - \Gamma^2\sigma_k^2) - 2z_k}{(1 + \Gamma\sigma_k)^2} \right] \quad (\text{A.9})$$

and D represents the operator, $D = \sum_k \rho_k \partial / \partial \rho_k = \rho_S \partial / \partial \rho_S$.

When the ion size and the permittivity are given by Eq. (40), then one has,

$$D(\sigma) = \sigma - \sigma^{(0)} \quad \text{and} \quad \varepsilon D(\varepsilon^{-1}) = 1 - \varepsilon / \varepsilon_w \quad (\text{A.10})$$

In the restricted case where all ions have the same diameter σ , then $\eta = 0$ and one gets an explicit result for Γ ,

$$\Gamma = \left[(1 + 2\kappa\sigma)^{1/2} - 1 \right] / (2\sigma) \quad (\text{A.11})$$

and

$$\ln \gamma^{MSA} = -\lambda \frac{\Gamma}{1 + \Gamma\sigma} \frac{1}{\rho_t} \sum_k \rho_k z_k^2 \quad \phi^{MSA} = -\frac{\Gamma^3}{3\pi\rho_t} \quad (\text{A.12})$$

It should be noted that no Born-like contribution is included in the expressions for γ and ϕ within the MSA. Indeed such a term, accounting for changes in ion-solvent interactions with concentration, is irrelevant at MM level where only (effective) ion-ion interactions should be considered [46].

For the hard sphere contributions one has [33],

$$\ln \gamma^{HS} = \left(\frac{X_2^3}{X_0 X_3^2} - 1 \right) \ln \Delta + \frac{X_3}{\Delta} + \frac{3X_1 X_2 (2 - X_3)}{X_0 \Delta^2} + \frac{X_2^3 (1 + 2X_3 - X_3^2)}{X_0 X_3 \Delta^3} + \frac{1}{\rho_t} \sum_k \rho_k Q_k D(\sigma_k) \quad (\text{A.13})$$

with $X_n = (\pi/6) \sum \rho_k \sigma_k^3$, and after correction of a power of 3 for Δ in the penultimate term, and

$$\phi^{HS} = \frac{X_3}{\Delta} + 3 \frac{X_1 X_2}{X_0 \Delta^2} + X_2^3 \frac{3 - X_3}{X_0 \Delta^3} + \frac{1}{\rho_t} \sum_k \rho_k Q_k D(\sigma_k) \quad (\text{A.14})$$

with $Q_k = F_1 + 2F_2\sigma_k + 3F_3\sigma_k^2$, where F_1 , F_2 , and F_3 are functions of the X_n 's and are given in Ref. 33.

Appendix B. Radial distribution functions at contact

Most of the notations of Ref. 54 are adopted in this section.

The cation and the anion have the same diameter σ . One defines

$$\beta^* = \lambda/\sigma, \quad \rho^* = \rho_t \sigma^3, \quad \eta = \frac{\pi}{6} \rho^*, \quad \Gamma^* = \Gamma\sigma \quad (\text{B.1})$$

where Γ is given by Eq. (A.11) and

$$Z = 1 + \frac{4\eta - 2\eta^2}{(1 - \eta)^3} + \rho^* \frac{\partial(\beta A^{ex}/N)}{\partial \rho^*} \quad (\text{B.2})$$

$$\beta A^{ex}/N = -\beta^* \frac{\Gamma^*}{1 + \Gamma^*} + \frac{(\Gamma^*)^3}{3\pi\rho^*} - B \quad (\text{B.3})$$

$$B = \frac{1}{128}[B_1 - B_2 \exp(-2\Gamma^*)] \quad (\text{B.4})$$

$$B_1 = 40 \frac{(\Gamma^*)^3}{3} - 12(\Gamma^*)^2 + 6\Gamma^* + 4 \quad (\text{B.5})$$

$$B_2 = 4(4\Gamma^* + 1) + (4\Gamma^* + 1) \sin(2\Gamma^*) - 4\Gamma^* \cos(2\Gamma^*) \quad (\text{B.6})$$

$$\beta U^{ex}/N = -\beta^* \frac{\Gamma^*}{1 + \Gamma^*} - \beta^* \frac{\partial B}{\partial \beta^*} \quad (\text{B.7})$$

The derivatives in Eqs. (B.2) and (B.7) were calculated using Maple.

With these definitions, the like and unlike RDF's at contact are expressed as,

$$g_{++}^c = g_{--}^c = \frac{1 + \eta/2}{(1 - \eta)^2} \exp(g_D^{MSA}) \quad (\text{B.8})$$

with

$$g_D^{MSA} = -\frac{\beta^*}{(1 + \Gamma^*)^2} \quad (\text{B.9})$$

and

$$g_{+-}^c = 2g_S - g_{++}^c \quad (\text{B.10})$$

with

$$g_S = 3[Z - 1 - (\beta U^{ex}/N)/3] / (2\pi\rho^*) \quad (\text{B.11})$$

It was checked within Maple that the numerical results of Ref. 54 for g_{++}^c and g_{+-}^c were recovered by using these relations.

References

- [1] P. Srikuhirin, S. Aphornratana, S. Chungpaibulpatana, A review of absorption refrigeration technologies, *Renew. Sust. Energ. Rev.* 5 (2001) 343–372. doi:10.1016/S1364-0321(01)00003-X.
- [2] Y. Zhang, C.-C. Chen, Thermodynamic modeling for CO₂ absorption in aqueous MDEA solution with Electrolyte NRTL model, *Ind. Eng. Chem. Res.* 50 (1) (2011) 163–175. doi:10.1021/ie1006855.
- [3] E. Lange, A. Robinson, The heats of dilution of strong electrolytes, *Chem. Rev.* 9 (1931) 89–116. doi:10.1021/cr60032a004.
- [4] T. W. Richards, A. W. Rowe, An indirect method of determining the specific heat of dilute solutions, with preliminary data concerning hydrochloric acid., *J. Am. Chem. Soc.* 42 (1920) 1621–1635. doi:10.1021/ja01453a013.
- [5] V. B. Parker, Thermal properties of aqueous uni-univalent electrolytes, Tech. rep., National Institute of Standards and Technology, Gaithersburg, MD (1965). doi:10.6028/NBS.NSRDS.2.
- [6] J. M. Sturtevant, The heat of dilution of aqueous hydrochloric acid at 25°, *J. Am. Chem. Soc.* 62 (1940) 584–587. doi:10.1021/ja01860a043.
- [7] C. E. Vanderzee, J. A. Swanson, Heats of dilution and relative apparent molal enthalpies of aqueous sodium perchlorate and perchloric acid, *J. Phys. Chem.* 67 (1963) 285–291. doi:10.1021/j100796a017.

- [8] F. Jones, R. Wood, The enthalpy and entropy of dilution of lithium perchlorate, *J. Phys. Chem.* 67 (1963) 1576–1578. doi:10.1021/j100802a003.
- [9] R. H. Wood, F. Belkin, Enthalpy and entropy of dilution of tetraethanolammonium bromide, *J. Chem. Eng. Data* 18 (1973) 184–186. doi:10.1021/je60057a020.
- [10] L. J. Gier, C. E. Vanderzee, Enthalpies of dilution and relative apparent molar enthalpies of aqueous calcium and manganous perchlorates, *J. Chem. Eng. Data* 19 (1974) 323–325. doi:10.1021/je60063a020.
- [11] E. Messikomer, R. Wood, The enthalpy of dilution of aqueous sodium chloride at 298.15 to 373.15 K, measured with a flow calorimeter, *J. Chem. Thermodyn.* 7 (1975) 119–130. doi:10.1016/0021-9614(75)90259-1.
- [12] H. P. Snipes, C. Manly, D. D. Ensor, Heats of dilution of aqueous electrolytes. Temperature dependence, *J. Chem. Eng. Data* 20 (1975) 287–291. doi:10.1021/je60066a027.
- [13] Y. Wu, T. Young, Enthalpies of dilution of aqueous electrolytes: sulfuric acid, hydrochloric acid, and lithium chloride, *J. Res. Natl. Bur. Stand.* 85 (1980) 11. doi:10.6028%2Fjres.085.002.
- [14] W. Guan, W.-F. Xue, S.-p. Chen, D.-W. Fang, Y. Huang, S.-L. Gao, Enthalpy of dilution of aqueous [C4mim][Gly] at 298.15 K, *J. Chem. Eng. Data* 54 (2009) 2871–2873. doi:10.1021/je8009539.
- [15] N. Bjerrum, Die Verdünnungswärme einer Ionenlösung in der Theorie von Debye und Hückel, *Z. Phys. Chem.* 119 (1926) 145–160. doi:10.1515/zpch-1926-11919.
- [16] G. Scatchard, Thermal expansion and the Debye-Hückel heat of dilution, *J. Am. Chem. Soc.* 53 (1931) 2037–2039. doi:10.1021/ja01357a002.
- [17] E. Guggenheim, J. Prue, Heats of dilution of aqueous electrolyte solutions, *Trans. Faraday Soc.* 50 (1954) 710–718. doi:10.1039/TF9545000710.
- [18] H. Schönert, The Debye-Hückel theory for hydrated ions. V. Enthalpy of aqueous solutions of alkali halides at 25° C, *Ber. Bunsenges. Phys. Chem.* 97 (1993) 64–69. doi:10.1002/bbpc.19930970113.
- [19] L. F. Silvester, K. S. Pitzer, Thermodynamics of electrolytes. 8. High-temperature properties, including enthalpy and heat capacity, with application to sodium chloride, *J. Phys. Chem.* 81 (1977) 1822–1828. doi:10.1021/j100534a007.
- [20] L. Blum, Simple electrolytes in the mean spherical approximation, in: H. Eyring, D. Henderson (Eds.), *Theoretical Chemistry, Advances and Perspectives*, Vol. 5, Academic Press: New York, 1980, pp. 1–66.
- [21] J. Barthel, J. Kröner, Heat of dilution of electrolyte solutions. Experimental method and data analysis, *J. Mol. Liq.* 81 (1999) 47–61. doi:10.1016/S0167-7322(99)00031-8.
- [22] J. M'halla, S. M'halla, G. Wipff, Analysis of experimental heats of dilution of aqueous solutions of NaBPh₄ by use of the mean spherical approximation and molecular dynamics simulations, *Chem. Phys.* 288 (2003) 1–22. doi:10.1016/S0301-0104(02)01019-4.

- [23] J. L. Oscarson, B. Liu, R. M. Izatt, A model incorporating ion dissociation, solute concentration, and solution density effects to describe the thermodynamics of aqueous sodium chloride solutions in the critical region of water, *Ind. Eng. Chem. Res.* 43 (2004) 7635–7646. doi:10.1021/ie040112p.
- [24] J.-P. Simonin, O. Bernard, N. Papaiconomou, W. Kunz, Description of dilution enthalpies and heat capacities for aqueous solutions within the msa–nrtl model with ion solvation, *Fluid Phase Equilib.* 264 (2008) 211–219. doi:10.1016/j.fluid.2007.11.018.
- [25] W. G. McMillan, J. E. Mayer, The statistical thermodynamics of multicomponent systems, *J. Chem. Phys.* 13 (1945) 276–305. doi:10.1063/1.1724036.
- [26] H. L. Friedman, Lewis-Randall to McMillan-Mayer conversion for the thermodynamic excess functions of solutions. Part I. Partial free energy coefficients, *J. Solution Chem.* 1 (1972) 387–412. doi:10.1007/BF00645603.
- [27] J. H. van’t Hoff, Die Rolle des osmotischen Druckes in der Analogie zwischen Lösungen und Gasen, *Z. Phys. Chem.* 1 (1887) 481–508. doi:doi:10.1515/zpch-1887-0151.
- [28] H. L. Friedman, Lewis-Randall to McMillan-Mayer conversion for the thermodynamic excess functions of solutions. Part II. Excess energy and volume, *J. Solution Chem.* 1 (1972) 413–417. doi:10.1007/BF00645604.
- [29] B. A. Pailthorpe, D. J. Mitchell, B. W. Ninham, Ion–solvent interactions and the activity coefficients of real electrolyte solutions, *J. Chem. Soc. Faraday Trans. 2* 80 (1984) 115–139. doi:10.1039/F29848000115.
- [30] J.-P. Simonin, Study of experimental-to-McMillan–Mayer conversion of thermodynamic excess functions, *J. Chem. Soc. Faraday Trans.* 92 (1996) 3519–3523. doi:10.1039/FT9969203519.
- [31] D. D. Ensor, H. L. Anderson, Heats of dilution of sodium chloride. temperature dependence, *J. Chem. Eng. Data* 18 (1973) 205–212.
- [32] K. S. Pitzer, J. C. Peiper, R. H. Busey, Thermodynamic Properties of Aqueous Sodium Chloride Solutions, *J. Phys. Chem. Ref. Data* 13 (1984) 1–102. doi:10.1063/1.555709.
- [33] J.-P. Simonin, L. Blum, P. Turq, Real ionic solutions in the mean spherical approximation. 1. Simple salts in the primitive model, *J. Phys. Chem.* 100 (1996) 7704–7709. doi:10.1021/jp953567o.
- [34] G. Rushbrooke, On the statistical mechanics of assemblies whose energy-levels depend on the temperature, *Trans. Faraday Soc.* 36 (1940) 1055–1062. doi:10.1039/TF9403601055.
- [35] J. C. Rasaiah, H. L. Friedman, Integral equation computations for aqueous 1–1 electrolytes. Accuracy of the method, *J. Chem. Phys.* 50 (9) (1969) 3965–3976. doi:10.1063/1.1671657.
- [36] J.-P. Hansen, I. R. McDonald, *Theory of simple liquids*, Academic Press, 2006.
- [37] T. Boublik, Hard sphere equation of state, *J. Chem. Phys.* 53 (1970) 471–472. doi:10.1063/1.1673824.

- [38] J. Salacuse, G. Stell, Polydisperse systems: Statistical thermodynamics, with applications to several models including hard and permeable spheres, *J. Chem. Phys.* 77 (1982) 3714–3725. doi:10.1063/1.444274.
- [39] L. Blum, J. S. Høye, Mean spherical model for asymmetric electrolytes. 2. Thermodynamic properties and the pair correlation function, *J. Phys. Chem.* 81 (13) (1977) 1311–1316. doi:10.1021/j100528a019.
- [40] J.-P. Simonin, Real ionic solutions in the mean spherical approximation. 2. Pure strong electrolytes up to very high concentrations, and mixtures, in the primitive model, *J. Phys. Chem. B* 101 (1997) 4313–4320. doi:10.1021/jp970102k.
- [41] J.-P. Simonin, O. Bernard, L. Blum, Real ionic solutions in the mean spherical approximation. 3. Osmotic and activity coefficients for associating electrolytes in the primitive model, *J. Phys. Chem. B* 102 (1998) 4411–4417. doi:10.1021/jp9732423.
- [42] L. G. Sillen, A. E. Martell, Stability constants of metal-ion complexes. Section 1, London Chemical Society, 1964.
- [43] H. Ohtaki, T. Radnai, Structure and dynamics of hydrated ions, *Chem. Rev.* 93 (1993) 1157–1204. doi:10.1021/cr00019a014.
- [44] H. F. Gibbard Jr, G. Scatchard, Liquid-vapor equilibrium of aqueous lithium chloride, from 25° to 100°C and from 1.0 to 18.5 molal, and related properties, *J. Chem. Eng. Data* 18 (1973) 293–298. doi:10.1021/jc60058a011.
- [45] J. S. Høye, J.-P. Simonin, Chemical potential of an ion in an asymmetric electrolyte within the mean spherical approximation (MSA)., *Mol. Phys.* 119 (2021) e1969045. doi:10.1080/00268976.2021.1969045.
- [46] J.-P. Simonin, Further reflections about the “Born” term used in thermodynamic models for electrolytes, *J. Mol. Liq.* 380 (2023) 121713. doi:10.1016/j.molliq.2023.121713.
- [47] J. Hubbard, L. Onsager, Dielectric dispersion and dielectric friction in electrolyte solutions. I., *J. Chem. Phys.* 67 (1977) 4850–4857. doi:10.1063/1.434664.
- [48] A. Chandra, Static dielectric constant of aqueous electrolyte solutions: Is there any dynamic contribution?, *J. Chem. Phys.* 113 (2000) 903–905. doi:10.1063/1.481870.
- [49] M. Sega, S. Kantorovich, A. Arnold, Kinetic dielectric decrement revisited: phenomenology of finite ion concentrations, *Phys. Chem. Chem. Phys.* 17 (2015) 130–133. doi:10.1039/C4CP04182H.
- [50] P. G. Wolynes, Dynamics of electrolyte solutions, *Ann. Rev. Phys. Chem.* 31 (1980) 345–376. doi:10.1146/annurev.pc.31.100180.002021.
- [51] C. Malmberg, A. Maryott, Dielectric constant of water from 0° to 100° C, *J. Res. Natl. Bur. Stand.* 56 (1956) 1–8. doi:10.6028/JRES.056.001.
- [52] P. Novotný, O. Šchnel, Densities of binary aqueous solutions of 306 inorganic substances, *J. Chem. Eng. Data* 33 (1988) 49–55. doi:10.1021/jc00051a018.
- [53] D. Chandler, Structures of molecular liquids, *Ann. Rev. Phys. Chem.* 29 (1978) 441–471. doi:10.1146/annurev.pc.29.100178.002301.

- [54] Q. Xu, K. Wu, J. Mi, C. Zhong, Improved radial distribution functions for Coulomb charged fluid based on first-order mean spherical approximation, *J. Chem. Phys.* 128 (2008) 214508. doi:10.1063/1.2931938.
- [55] J.-P. Simonin, O. Bernard, Insight into the ionic atmosphere effect: Comparison of theories for electrolytes at the primitive level, *Fluid Phase Equilib.* 571 (2023) 113805. doi:10.1016/j.fluid.2023.113805.